

## In Silico-Guided Target Identification of a Scaffold-Focused Library: 1,3,5-Triazepan-2,6-diones as Novel Phospholipase A2 Inhibitors

Pascal Muller,<sup>†</sup> Gersande Lena,<sup>‡</sup> Eric Boilard,<sup>||</sup> Sofiane Bezzine,<sup>||,§</sup> Gérard Lambeau,<sup>||</sup> Gilles Guichard,<sup>‡</sup> and Didier Rognan<sup>†,\*</sup>

Bioinformatics of the Drug, CNRS UMR 7175, F-67400 Illkirch, and Immunologie et Chimie Thérapeutiques, CNRS UPR 9021, Institut de Biologie Moléculaire et Cellulaire (IBMC), F-67084 Strasbourg Cedex, France, and Institut de Pharmacologie Moléculaire et Cellulaire, CNRS UMR 6097, F-06560 Valbonne, France

Received June 2, 2006

A collection of 2150 druggable active sites from the Protein Data Bank was screened by high-throughput docking to identify putative targets for five representative molecules of a combinatorial library sharing a 1,3,5-triazepan-2,6-dione scaffold. Five targets were prioritized for experimental evaluation by computing enrichment in individual protein entries among the top 2% scoring targets. Out of the five proposed proteins, secreted phospholipase A2 (sPLA2) was shown to be a true target for a panel of 1,3,5-triazepan-2,6-diones which exhibited micromolar affinities toward two human sPLA2 members.

### Introduction

To optimize the chances of developing new drugs, academia and the pharmaceutical industry have developed numerous strategies<sup>1,2</sup> to identify both interesting targets and ligands at a high-throughput level. Among the many possible scenarios, there is an increasing need to characterize the target(s) of a known bioactive ligand. First, a hit/lead can be identified by high-content screening (metabolic pathways,<sup>3</sup> in cellulo,<sup>4</sup> phenotypic screening<sup>5</sup>) or serendipity,<sup>6</sup> but target identification is required to guide its optimization. Second, addressing both potency and selectivity of a known ligand is increasingly addressed in an early lead optimization phase. Selectivity within a target family (e.g. GPCRs, kinases), toward proteins unrelated to the main target or even antitargets, currently represent strategic information for lead prioritization.<sup>7</sup> Third, ligand libraries<sup>8</sup> focused on new molecular scaffolds become available from academic or commercial sources for high-throughput screening. However, whether this new chemical space overlaps target space is unknown and prioritizing the most likely targets of such new libraries might be of interest in order to make a decision regarding their purchase.

The experimental determination at a precise molecular level of a molecular target for a given ligand is still a cumbersome and difficult task. Many directions may be followed going from simple target screening to various “-omics” strategies.<sup>9</sup> Regarding the huge chemical space covered by all druggable targets,<sup>10</sup> computational approaches may help to prioritize the most likely target space to cover. Browsing compound libraries to identify ligands of interest and subsequently selecting their cognate enzymes/receptors as top priority targets to investigate is, for example, a simple and straightforward strategy. However, it requires a significant overlap between the real target and targets with known ligands and therefore might fail for orphan receptors. Experimentally determined or computed binding

affinity fingerprints<sup>11–13</sup> may also be used to prioritize target selection. This approach is, however, heavily dependent on the diversity of experimental data (targets and compounds selected for deriving the binding affinity matrixes) and restricted to few protein subfamilies. Mathematical models designed to fit target space with ligand space by means of 2-D and 3-D descriptors have also been described<sup>14,15</sup> and been proven to recover the true targets of known ligands, but their utility in prospective studies still needs to be demonstrated.

Last, serial docking of ligands to a few related targets can be used to select the binding sites that look the most complementary to the ligand of interest.<sup>16,17</sup> Surprisingly, high-throughput docking to protein binding sites has rarely been used to address the problem of target identification and prediction of putative site effects.<sup>18–20</sup> Although it uses the same paradigm as ligand screening (predicting the most likely ligand–target interactions from molecular docking), docking a single ligand to a target library is more difficult to setup than classical docking of a ligand library to a single target.

It first requires an annotated target library for which binding sites have clearly been identified. We therefore chose the Protein Data Bank (PDB)<sup>21</sup> for that purpose since it contains high-resolution 3-D data. Customizing a reliable target library from the PDB is, however, far from being trivial because of the extraordinary heterogeneity of this dataset. One of the key issues is to automatically detect the most interesting binding sites either on the fly<sup>22,23</sup> or from the 3-D coordinates of bound ligands.<sup>20,24–26</sup> Then, binding sites must be analyzed in order to keep only those able to topologically accommodate a ‘drug-like’ ligand. Several collections of protein binding sites have been described recently.<sup>20,27,28</sup> Only two of them (Binding MOAD<sup>26</sup> and sc-PDB<sup>20,24</sup>) discriminate between druggable (accommodating a drug-like ligand) and nondruggable (accommodating ions, solvents, or detergents) binding sites. In the current study, the in-house-developed sc-PDB target library<sup>20,24</sup> was chosen because both protein and active site coordinates have already been processed (addition of hydrogen atoms, removal of solvent, and catalytically unimportant ions) and are ready for docking.

Second, one should automate the generation of input files (3-D coordinates of the target and/or of the cognate binding site; docking configuration file) for a large array of heterogeneous targets, which is much more difficult than setting up a reliable set of coordinates for a ligand library. Notably, protein

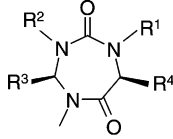
\* Corresponding author. Phone: +333.90244235. Fax: +333.90244310. E-mail: didier.rognan@pharma.u-strasbg.fr.

<sup>†</sup> Bioinformatics of the Drug, CNRS UMR 7175, Institut de Biologie Moléculaire et Cellulaire.

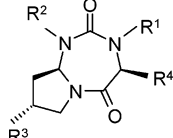
<sup>‡</sup> Immunologie et Chimie Thérapeutiques, CNRS UPR 9021, Institut de Biologie Moléculaire et Cellulaire.

<sup>||</sup> Institut de Pharmacologie Moléculaire et Cellulaire.

<sup>§</sup> Present address: Laboratoire de Biochimie et de Génie Enzymatique des Lipases, ENIS, BP“W”, 3038 Sfax-Tunisia.

**Table 1.** Structure of 1,3,5-Triazepan-2,6-diones **1–26**


compound	R <sup>1</sup>	R <sup>2</sup>	R <sup>3</sup>	R <sup>4</sup>
1	H	H	H	CH <sub>2</sub> Ph
2	H	CH <sub>2</sub> Ph	H	CH <sub>2</sub> Ph
3	H	CH <sub>2</sub> COOCH <sub>3</sub>	H	CH <sub>2</sub> Ph
4	H	CH <sub>2</sub> COO <i>t</i> Bu	H	CH <sub>2</sub> Ph
5	H	CH <sub>2</sub> COOH	H	CH <sub>2</sub> Ph
6	H	CH <sub>2</sub> CH <sub>2</sub> OH	H	CH <sub>2</sub> Ph
7	H	CH <sub>2</sub> CHO	H	CH <sub>2</sub> Ph
8	H	CH <sub>2</sub> CH=CH-COO <i>t</i> Bu	H	CH <sub>2</sub> Ph
9	H	(CH <sub>2</sub> ) <sub>3</sub> -COO <i>t</i> Bu	H	CH <sub>2</sub> Ph
10	H	(CH <sub>2</sub> ) <sub>3</sub> -COOH	H	CH <sub>2</sub> Ph
11	H	(CH <sub>2</sub> ) <sub>3</sub> -CONH <sub>2</sub>	H	CH <sub>2</sub> Ph
12	H	CH <sub>2</sub> CONH <sub>2</sub>	H	CH <sub>2</sub> Ph
13	H	CH <sub>2</sub> CH=CH-COOH	H	CH <sub>2</sub> Ph
14	H	H	H	<i>i</i> Bu
15	H	H	H	CH <sub>2</sub> NHFmoc
16	H	H	H	CH <sub>2</sub> NH <sub>2</sub>
17	H	H	H	Ph
18	H	H	H	<i>i</i> Pr
19	H	CH <sub>2</sub> COO <i>t</i> Bu	H	<i>i</i> Pr
20	H	CH <sub>2</sub> Ph	H	<i>i</i> Pr
21	H	H	CH <sub>2</sub> Ph	CH <sub>2</sub> Ph
22	H	H	H	CH <sub>2</sub> -βNaphthyl
23	H	CH <sub>2</sub> COO <i>t</i> Bu	H	CH <sub>2</sub> -βNaphthyl
24	CH <sub>2</sub> Ph	CH <sub>2</sub> Ph	H	CH <sub>2</sub> Ph
25	CH <sub>2</sub> COOH	CH <sub>2</sub> COOH	H	CH <sub>2</sub> Ph
26	CH <sub>2</sub> COO <i>t</i> Bu	CH <sub>2</sub> COO <i>t</i> Bu	H	CH <sub>2</sub> Ph

**Table 2.** Structure of 1,3,5-Triazepan-2,6-diones **27–34**


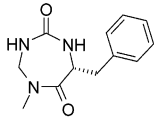
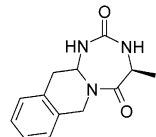
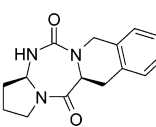
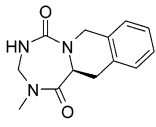
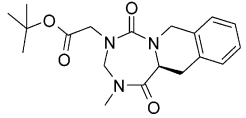
compound	R <sup>1</sup>	R <sup>2</sup>	R <sup>3</sup>	R <sup>4</sup>
27	H	H	H	CH <sub>2</sub> Ph
28	H	H	O-CH <sub>2</sub> Ph	CH <sub>2</sub> Ph
29	H	H	OH	CH <sub>2</sub> Ph
30	H	H	H	CH <sub>2</sub> -βNaphthyl
31	H	CH <sub>2</sub> COO <i>t</i> Bu	H	CH <sub>2</sub> Ph
32	CH <sub>2</sub> COO <i>t</i> Bu	CH <sub>2</sub> COO <i>t</i> Bu	H	CH <sub>2</sub> Ph
33	H	CH <sub>2</sub> Ph	H	CH <sub>2</sub> Ph
34	H	CH <sub>2</sub> COO <i>t</i> Bu	H	CH <sub>2</sub> -βNaphthyl

and binding site 3-D coordinates should be prepared automatically and suitable for docking by removal of any additional molecule (solvent, ion, and cofactor) not essential for ligand binding. We have chosen the GOLD docking software<sup>29</sup> for two main reasons: (i) it is one of the most robust and accurate docking tool in our hands;<sup>30</sup> (ii) it only requires a single configuration file (gold.conf) whose distribution over a target library is easy to automate.

Last, the annotation of the target library is desirable in order to facilitate either target selection for screening or postprocessing docking data according to enrichment plots. We already reported an automated annotation procedure for PDB entries resulting in the definition of several attributes (e.g. EC number, protein name, species, resolution, thermal factors, and ligand) for each binding cavity.<sup>24,31</sup>

In a recent report,<sup>20</sup> we demonstrated the proof-of-concept of this inverse screening approach that was able to recover the known target(s) of chemically dissimilar ligands with up to 100-fold enrichment over random picking. Herewith, we describe

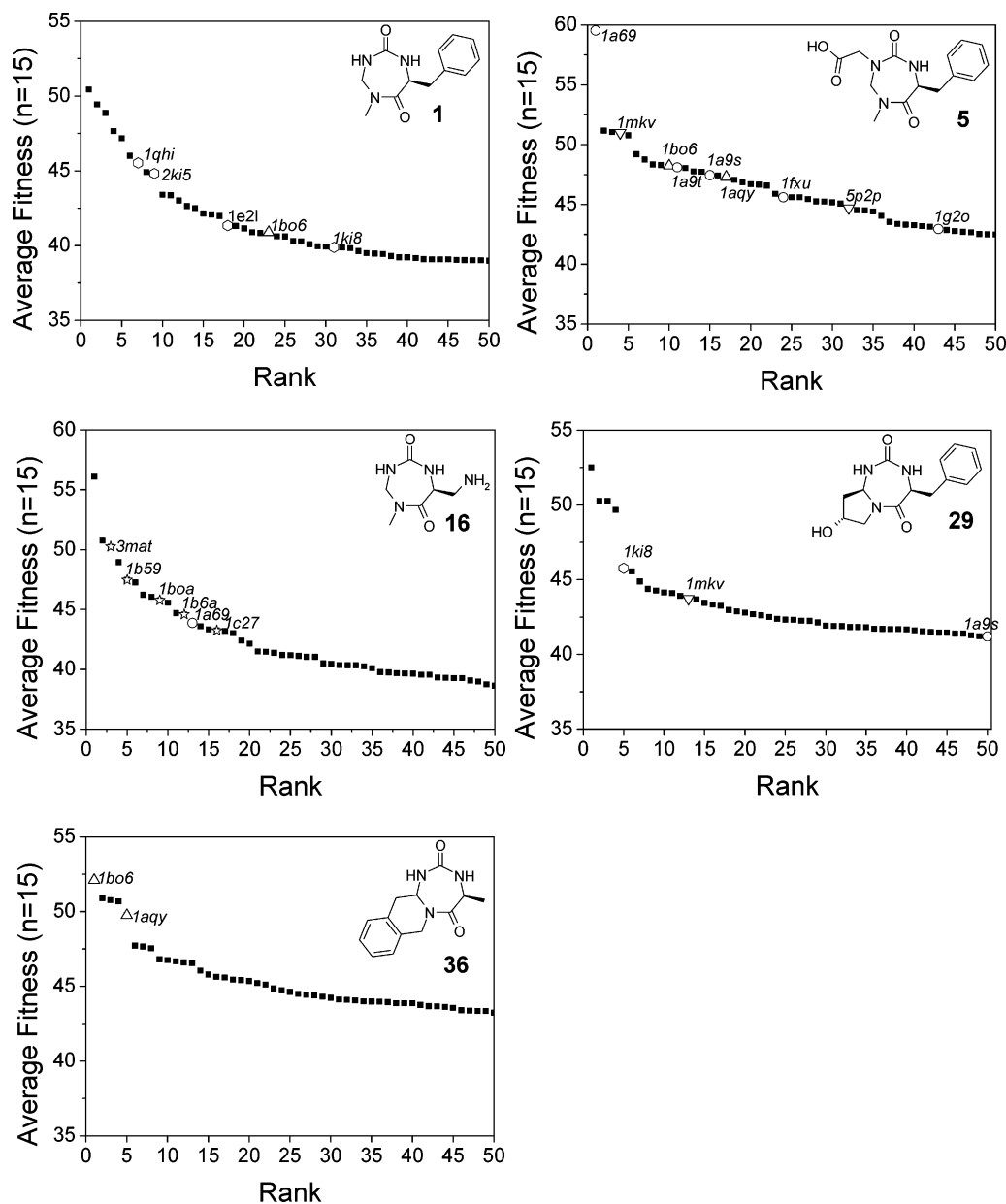
**Table 3.** Structure of 1,3,5-Triazepan-2,6-diones **35–39**

Compound	Structure
35	
36	
37	
38	
39	

the application of inverse docking to the identification of the most likely targets of a panel of new drug-like compounds derived from a scaffold-focused combinatorial library. To the best of our knowledge, this is the first report of an *in silico*-guided target identification for drug-like compounds. The simplicity of the approach makes it particularly attractive for prioritizing a few targets for experimental validation and is therefore a good complement to experimental target identification strategies.

## Results

**Virtual Screening of the sc-PDB Protein Library.** A collection of 2148 binding sites extracted from the Protein Data Bank has been screened by high-throughput docking to predict the most likely targets of five compounds representative of the herein presented combinatorial library (**1**, **5**, **16**, **29**, **36**; Tables 1–3). In the sc-PDB dataset,<sup>31</sup> a target is defined either as an enzyme from the PDB with a unique EC number, or a nonenzymatic protein with a unique name according to our previous annotation of the database. Differences related to species, isoforms, or mutations are thus not considered in our classification scheme. For each of the five investigated compounds, a target was selected if it fulfilled any of the three following criteria: (i) 50% of target entries present in the sc-PDB were scored, according to the average GOLD fitness score, among the top 2% scoring entries; (ii) two entries of the same target were scored in the top 2% scoring entries; (iii) the average fitness score for all entries of the corresponding target was above 50. This selection protocol afforded a final list of nine enzymes (Table 4) which collectively describe the targets which could accommodate the triazepandione chemotype. Out of these nine targets, four (aconitase, D-amino acid oxidase, lypopolysaccharide 3-α-galactosyl transferase, hypoxanthine-guanine phosphoribosyl transferase; Table 4) were not further investigated because of either a lack of therapeutic relevance or the impossibility to proceed with an inhibition assay. Five remaining



**Figure 1.** Averaged fitness score of sc-PDB entries for compounds **1**, **5**, **16**, **29**, and **36**. PDB entries are ranked by decreasing GOLD fitness score. Target entries selected for biological evaluation (see Experimental Section) are indicated by up-triangles (estrogen sulfotransferase), down-triangles (phospholipase A2), circles (purine nucleoside phosphorylase), stars (methionine aminopeptidase), and diamonds (thymidine kinase).

**Table 4.** Predicted Targets for Compounds **1**, **5**, **16**, **29**, and **36**

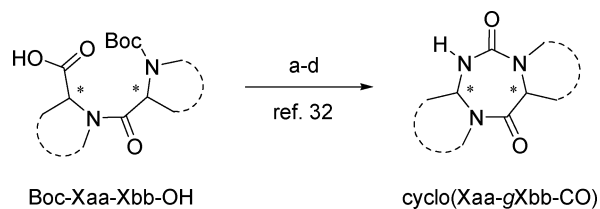
target	EC number <sup>a</sup>	N <sup>b</sup>	target rate, % <sup>c</sup>				
			1	5	16	29	36
aconitase	4.2.1.3	7	43			29	
DAAO <sup>d</sup>	1.4.3.3	2	50			50	
EST <sup>e</sup>	2.8.2.4	2	50	100	50		
GT <sup>f</sup>	2.4.1	2		50		100	
HPRT <sup>g</sup>	2.4.2.8	6		17		33	
MA <sup>h</sup>	3.4.11.18	5				20	100
PLA2 <sup>i</sup>	3.1.1.4	8		25		13	
PNP <sup>j</sup>	2.4.2.1	6		83			
TK <sup>k</sup>	2.7.1.21	5	80			20	

<sup>a</sup> Enzyme commission number.<sup>61</sup> <sup>b</sup> Number of sc-PDB entries describing the target. <sup>c</sup> Target rate: Percentage of targets ranked in the top 2% scoring entries. <sup>d</sup> D-amino acid oxidase. <sup>e</sup> Estrogen sulfotransferase. <sup>f</sup> Lipopolysaccharide 3- $\alpha$ -galactosyltransferase. <sup>g</sup> Hypoxanthine-guanine phosphoribosyltransferase. <sup>h</sup> Methionine aminopeptidase. <sup>i</sup> Phospholipase A2. <sup>j</sup> Purine nucleoside phosphorylase. <sup>k</sup> Thymidine kinase.

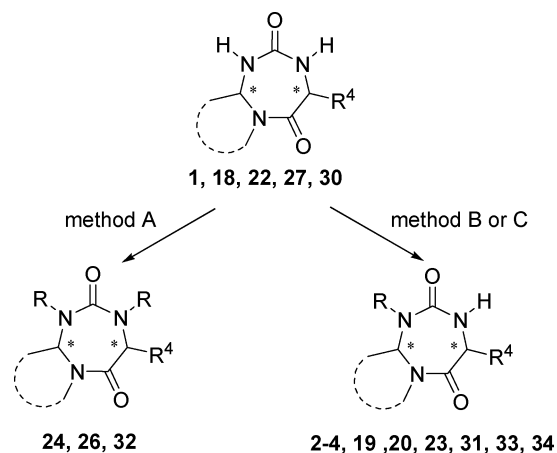
targets, estrogen sulfotransferase (EST), methionine aminopeptidase (MA), secreted phospholipase A2 (sPLA2), purine

nucleoside phosphorylase (PNP), and thymidine kinase (TK) were finally retained and predicted to bind at at least two out of the five screened compounds (Table 4, Figure 1). Figure 1 indicates which PDB entries have precisely been selected by each of the five compounds. Compounds **5** and **29** were predicted to be rather permissive for three targets (Figure 1), the three other reference compounds exhibiting a strong preference for a single enzyme (TK for compound **1**, MA for compound **16**, EST for compound **36**; Figure 1).

**Synthesis.** The general synthetic approach to 1,3,5-triazepan-2,6-diones has been described previously.<sup>32</sup> Briefly, the 1,3,5-triazepan-2,6-dione skeleton cyclo(Xaa-gXbb-CO)<sup>33</sup> was constructed in four steps by cyclization of simple dipeptide-derived precursors (Scheme 1). The synthesis involved Curtius rearrangement of N-protected dipeptidyl azides prepared from the corresponding starting dipeptide Boc-Xaa-Xbb-OH. The resulting dipeptidyl isocyanates were treated with N-hydroxysuccinimide to afford N-Boc protected succinimidyl carbamate derivatives as key intermediates. The Boc group was selectively

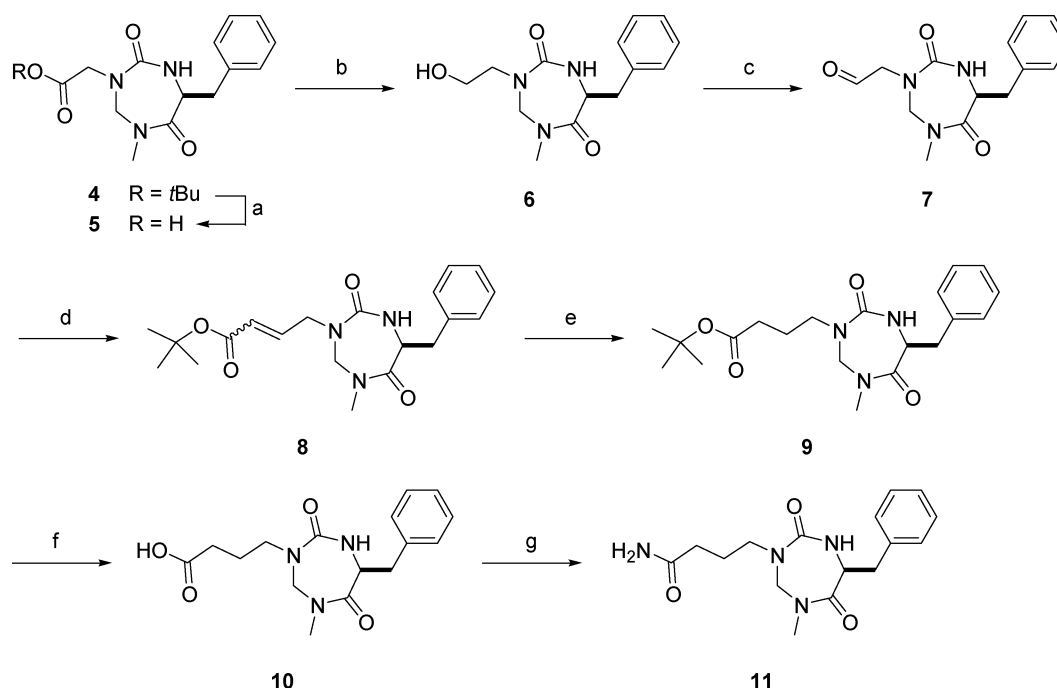
Scheme 1<sup>a</sup>

<sup>a</sup> (a) EtOCOCI, NMM, THF,  $-20^{\circ}\text{C}$ , then  $\text{NaN}_3$  in  $\text{H}_2\text{O}$ ; (b) toluene,  $65^{\circ}\text{C}$ , then HOSu and pyridine; (c) TFA, 30 min; (d) DIPEA, MeCN.

Scheme 2<sup>a</sup>

<sup>a</sup> Method A: NaH (4 equiv), RX (4 equiv), THF, 48 h; method B:  $\text{KF}/\text{Al}_2\text{O}_3$  40 wt % (10 equiv), RX (1.5 equiv),  $\text{CH}_2\text{Cl}_2$  or THF, 24–96 h; method C: NaH (2 equiv), RX (1.5 equiv),  $\text{CH}_2\text{Cl}_2$ , 24 h.

removed by treatment with trifluoroacetic acid (TFA) and the resulting TFA salt cyclized to the 1,3,5-triazepan-2,6-dione in the presence of diisopropylethylamine (DIPEA). Treatment of cyclo(Xaa-gXbb-CO) with NaH (5 equiv) and various electrophiles (3 equiv) (method A) afforded dialkylated cyclo-ureas

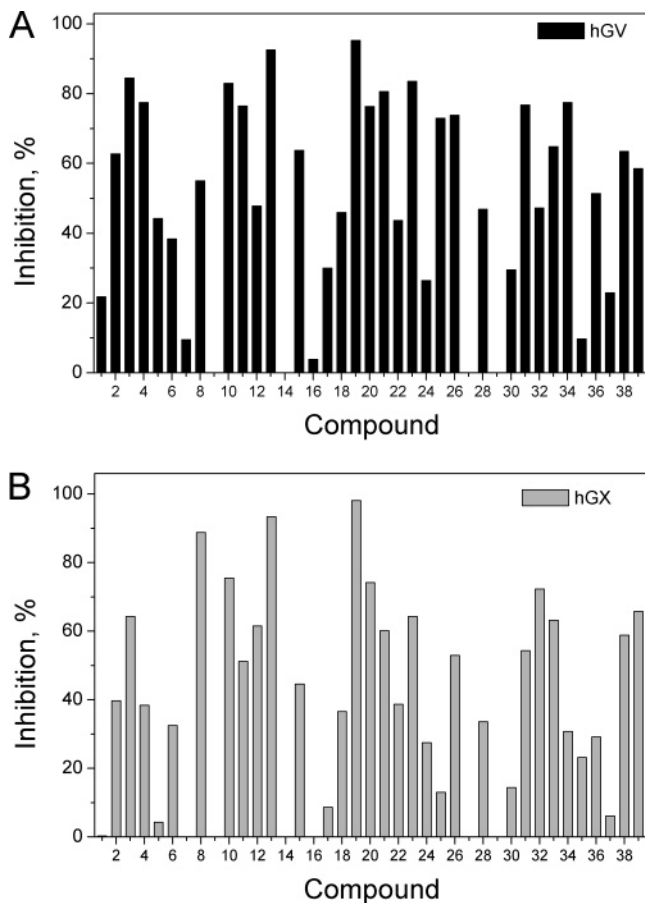
Scheme 3<sup>a</sup>

<sup>a</sup> (a) TFA; (b) NMM (1.2 equiv), THF,  $-20^{\circ}\text{C}$ ,  $t\text{BuOCOCI}$  (1.2 equiv), 25 min, r.t., 5 min,  $-20^{\circ}\text{C}$ ,  $\text{NaBH}_4$  (3 equiv), 20 min, 50%; (c)  $\text{COCl}_2$  (1.5 equiv),  $\text{CH}_2\text{Cl}_2$ ,  $-20^{\circ}\text{C}$ , DMSO (3 equiv), then DIPEA (6 equiv), 5 min, r.t.; (d)  $(\text{Ph})_3\text{PCHCOOtBu}$ ,  $\text{CH}_2\text{Cl}_2$ , r.t., 2 h 30 min, 70% over two steps; (e) Pd/C (10 wt %), EtOH, r.t., 16 h, 97%; (f) TFA, r.t., 30 min, 55%; (g) BOP (1.05 equiv), HOBT (1.05 equiv), DIPEA (3.15 equiv), Sieber resin (1.5 equiv), DMF, r.t., 1 h 30 min,  $\text{CH}_2\text{Cl}_2/\text{TFA}$  (9:1), r.t., 40 min, 68%.

24, 26, and 32 in yields ranging from 50 to 82% after silica gel chromatography (Scheme 2). Alternatively methods B and C allowed selective monoalkylation of 1,3,5-triazepan-2,6-diones at the *gem*-diamino urea nitrogen (e.g. 2–4, 19, 20, 23, 31, 33, 34) in yields ranging from 25 to 94%. Compound 11 was synthesized in seven steps from 3 (Scheme 3). The *tert*-butyl side chain of 3 was removed quantitatively by treatment with TFA to afford 5. The carboxylic acid function of 5 was reduced to the corresponding alcohol in 50% yield by treatment of its mixed anhydride with an aqueous solution of  $\text{NaBH}_4$ .<sup>34</sup> Swern oxidation of 6 gave aldehyde 7 which was engaged directly in a Wittig reaction. Reaction with (*tert*-butyloxycarbonylmethylene)triphenyl-phosphorane afforded 8 (70% yield for the two steps) as a mixture of *E* and *Z* isomers (*Z/E* ratio = 1:6). The hydrogenation of the double bond yielded 9 in 97% yield. Further removal of the *tert*-butyl group by treatment with TFA led to the corresponding carboxylic acid 10 in 55% yield. The optimized preparation of the amide 11 featured reaction of compound 10 with Sieber amide resin, i.e., 9-Fmoc-aminoxanthan-3-yloxy-Merrifield resin<sup>35</sup> (whose *N*-Fmoc protecting group was removed by treatment with a mixture of DMF/ piperidine 3:1), followed by cleavage with 10% TFA in  $\text{CH}_2\text{Cl}_2$ . The desired compound 11 was obtained in 68% yield, after purification by flash column chromatography. Similarly, treatment of acid 5 under the same conditions afforded amide 12 in 74% yield. A fraction of *tert*-butyl ester 8 (*E* isomer) was treated with TFA to provide 13 with  $\alpha,\beta$ -unsaturated carboxylic side chain in 54% yield.

**1,3,5-Triazepan-2,6-diones Are a New Class of Secreted Phospholipase A2 Inhibitors.** Preliminary binding assays were performed using a starting panel of nine compounds including the analogues screened by our *in silico* protocol (1, 5, 16, 29, and 36) plus four other compounds (14, 28, 33, and 37) which were physically available at the time of the experimental screening. For three of the five predicted targets (human EST,



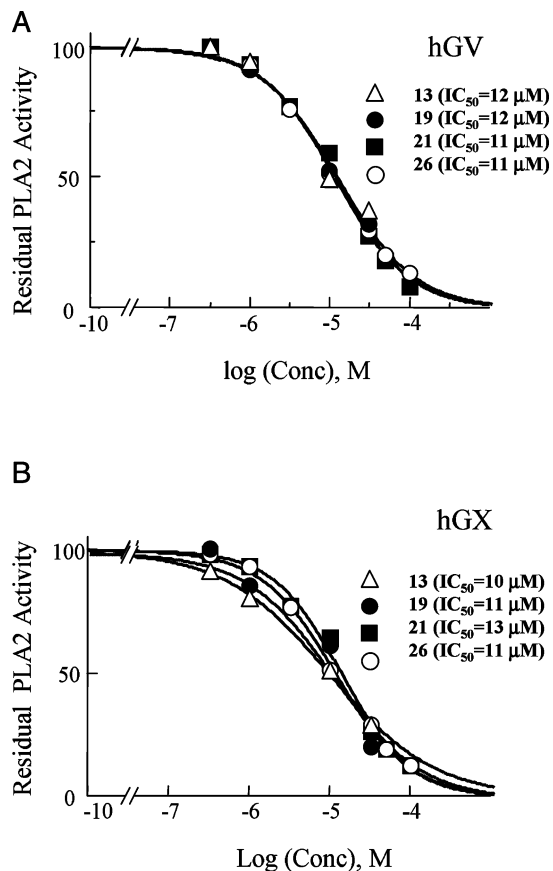


**Figure 2.** Inhibition of hGV (panel A) and hGX (panel B) sPLA2s by compounds 1–39 at 30  $\mu\text{M}$ . hGV (40 pM) or hGX (20 pM) sPLA2s were preincubated for 15 min with each compound, and the enzymatic assay was initiated by adding  $^3\text{H}$ -oleate-radiolabeled *E. coli* membranes as substrate.<sup>55</sup> Results are representative of at least three independent experiments.

Herpes simplex type-1 TK, AM), no inhibitory potency could be detected among the nine tested compounds even at high micromolar concentrations (not shown).

One target (PNP) gave ambiguous results since a single micromolar inhibitor (compound 28,  $K_i = 8 \mu\text{M}$ ) could be found for PNP from *Toxoplasma gondii* but none for the human PNP (data not shown). PNP was therefore discarded for further studies.

Last, we tested the nine above compounds for their potency to inhibit the enzymatic activity of several human secreted PLA2s (sPLA2s) at 10 and 100  $\mu\text{M}$ . These initial enzymatic assays showed that several compounds inhibited to a different extent the catalytic activity of human group IB, IIA, V, and X sPLA2s but had no effect on that of human group III sPLA2 (not shown). Interestingly, the different compounds appeared more potent on human group V (hGV) and human group X (hGX) sPLA2s. On the basis of these assays, we then tested a total of 38 triazepandione (Tables 1–3) compounds at 30  $\mu\text{M}$  on group IB, IIA, V, and X sPLA2s. All compounds showed only weak or no inhibition on group IB and IIA sPLA2s (not shown). Conversely, several of them were clearly inhibiting hGV and hGX sPLA2s (Figure 2). At a defined threshold of 70% inhibition, 13 compounds (3, 4, 10, 11, 13, 19, 20, 21, 23, 25, 26, 31, and 34) inhibited hGV sPLA2 whereas six compounds (8, 10, 13, 19, 20, and 32) significantly inhibited the enzymatic activity of hGX sPLA2. Four of the best compounds (13, 19, 21, 26) were further investigated and found to inhibit both hGV and hGX sPLA2s with  $\text{IC}_{50}$  values around 10  $\mu\text{M}$  (Figure 3).



**Figure 3.**  $\text{IC}_{50}$  values for compounds 13, 19, 21, 24, and 26 to hGV (panel A) and hGX (panel B) sPLA2s. hGV (40 pM) or hGX (20 pM) were preincubated for 15 min with the indicated compounds at various concentrations, and the enzymatic assay was started by adding  $^3\text{H}$ -oleate-radiolabeled *E. coli* membranes as substrate.<sup>55</sup> Results are representative of three independent experiments performed with two different batches of compounds.

## Discussion

Identifying the possible target(s) of a new chemotype is rendered very complex by the quantity of different screening setups that have to be addressed simultaneously. We herewith propose a simple and straightforward *in silico*-guided strategy aimed at prioritizing the most likely targets of compounds sharing the same molecular scaffold by systematically docking a few representative compounds to a set of druggable binding sites of known X-ray structure. When applied to the novel series of 1,3,5-triazepan-2,6-diones, a restricted set of targets could be prioritized, out of which two distinct human sPLA2s were demonstrated to be true targets for this new chemotype.

It should be acknowledged that, out of the two compounds (5 and 29) which enabled us to select sPLA2 as a putative target in our computational screen, only compound 5 presented some inhibitory potency for hGV (Figure 2). As a matter of fact, out of the eight PLA2 copies present in our target library, no entries described the experimentally identified sPLA2 targets (hGV and hGX). Indeed, hGV sPLA2 has not been crystallized so far, and only the crystal structure of apo hGX sPLA2<sup>36</sup> was available at the time of the *in silico* screening and thus was not stored in the sc-PDB database. All entries describing various isoforms of sPLA2 in release 1 of the sc-PDB<sup>20</sup> were for porcine and bovine group IB sPLA2s and for human group IIA sPLA2. For human group IB and IIA sPLA2s, no or only weak inhibitory potencies could be measured with compounds 5 and 29 (data not shown). For instance, compound 5 had no effect on human

**Table 5.** Predicted Targets for Compounds **13**, **19**, **21**, and **26**

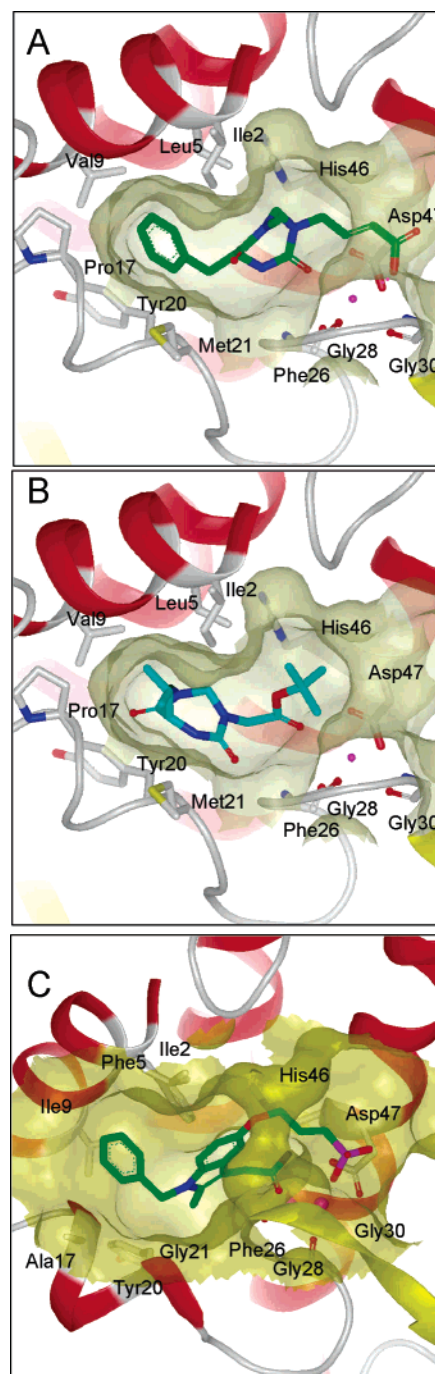
target	EC number <sup>a</sup>	N <sup>b</sup>	target rate, % <sup>c</sup>			
			13	19	21	26
MTAP <sup>d</sup>	2.4.2.28	5	40			
AChE <sup>e</sup>	3.1.1.7	6				33
CS1 <sup>f</sup>	1.14.11.21	2				100
MIF <sup>g</sup>	5.3.2.1	4				75
PLA2 <sup>h</sup>	3.1.1.4	8	13	25		
PNP <sup>i</sup>	2.4.2.1	6	16	16		
tK <sup>j</sup>	2.7.4.9	6	16	16	33	
TS <sup>k</sup>	4.2.1.20	13			46	

<sup>a</sup> Enzyme commission number.<sup>61</sup> <sup>b</sup> Number of sc-PDB entries describing the target. <sup>c</sup> Target rate: Percentage of targets ranked in the top 2% scoring entries. <sup>d</sup> MTAP: 5'-methylthioadenosine phosphorylase. <sup>e</sup> AChE: Acetylcholinesterase. <sup>f</sup> CS1: Clavaminate synthase 1. <sup>g</sup> MIF: Macrophage migration inhibitory factor. <sup>h</sup> PLA2: Phospholipase A2. <sup>i</sup> PNP: Purine nucleoside phosphorylase. <sup>j</sup> tK: Thymidylate kinase. <sup>k</sup> TS: Tryptophan synthase.

group IB sPLA2 while it inhibited only 25% of hGIIA sPLA2 activity at 30  $\mu$ M. However, the corresponding carboxylic esters (compounds **3** and **4**), although they are also modest inhibitors of hGIIA sPLA2, are much stronger inhibitors of group V and X sPLA2s (Figure 2). When the best inhibitors (compounds **13**, **19**, **21**, and **26**) were screened back against the sc-PDB target, sPLA2 was also recovered among the eight selected targets for two of the four compounds (Table 5). Therefore, our computational approach to deorphanize a compound series although not perfect is more likely to succeed if (i) several compounds describing the same chemotype are screened both *in silico* and experimentally, and (ii) multiple entries describing a family of proteins are stored in our target library. Possible misdocking arising from either particular ligands or active sites are thus statistically minimized if a series of congeneric compounds is docked to a series of congeneric binding sites.

Although the inhibitory potencies of our current triazepandione compounds are still relatively modest on hGV and hGX sPLA2s (Figure 3), these compounds appeared to be true competitive inhibitors.<sup>37</sup> First, we monitored the rate of alkylation of His46 at the catalytic site of hGV sPLA2 by *p*-bromophenacyl bromide<sup>37,38</sup> in the presence or absence of compound **19** and found that the presence of this compound leads to a significant increase in the half-time for inactivation of the enzyme by alkylation (not shown). The most likely explanation for this result is that binding of compound **19** to the sPLA2 catalytic site slows down the alkylation reaction by steric hindrance, as previously demonstrated for several sPLA2 competitive inhibitors.<sup>37</sup> Second, we found that this compound, when stoichiometrically complexed to hGV sPLA2, decreased its binding affinity for the M-type receptor target,<sup>39</sup> an effect which is likely due to a steric modulation of the sPLA2-receptor interaction (Boilard et al., manuscript in preparation). These findings appeared in accordance with the a posteriori docking experiments described below.

The predicted binding mode for two of the best sPLA2 inhibitors (compounds **13** and **19**) to the catalytic site of hGX sPLA2 (Figure 4) explains fairly well the observed structure–activity relationships (Table 1). First, compounds presenting carboxylic acid or ester moieties at R<sup>2</sup> were the most potent inhibitors since these groups are able to coordinate a catalytically important calcium ion of the binding site (Figure 4). The triazepandione core is embedded in the catalytic site of the enzyme, similarly to a known series of indole derivatives exemplified by indoxam.<sup>40,41</sup> The triazepandione scaffold is proposed to bind with two slightly translated binding modes depending on the nature of the R<sup>2</sup> substituent at N-3 (Table 1). Long chain carboxylic acid and esters (e.g. compounds **8**, **10**,



**Figure 4.** Predicted binding mode of compounds **13** (A), **19** (B) to hGX sPLA2 (modeled from the pdb entry 1le6) and X-ray structure of the inhibitor LY311727 (C) to hGIIA sPLA2 (pdb entry: 1db4). Compounds were built and docked as described for compounds **1**, **5**, **16**, **29**, and **36** in the Experimental Section, with the exception that both axial and equatorial positions were allowed at substituents R<sup>3</sup> and R<sup>4</sup>, as recently exemplified by the X-ray structure of compound **21**.<sup>32</sup> The main chain of sPLA2 is traced by red helices, yellow strands, and white loops. The ligand binding site is delimited by a solid surface. sPLA2-bound compounds **13** and LY311727 (green carbon atoms) and **19** (cyan carbon atoms) are displayed along with the neighboring protein side chains (white carbon atoms) and the catalytic calcium ion (magenta ball). Except for above-described carbon atoms, the color coding is as follows: nitrogen, blue; oxygen, red, sulfur, yellow; phosphorus, magenta.

**11**, and **13**) can directly coordinate the catalytic calcium ion at the vicinity of His46 and Asp47 (Figure 4) and place the triazepandione in the center of the binding site, the urea carbonyl moiety completing the prototypical heptacoordination of calcium

(Figure 4A). The preference for hydrophobic substituents (isopropyl, benzyl) at R<sup>4</sup> could be explained by the presence of a hydrophobic cage (Ile2, Leu5, Val9, Pro17, Tyr20, Met21) that nicely accommodates the R<sup>4</sup> group (Figure 4A,B). For shorter chains at R<sup>2</sup> (e.g. compounds **3**, **4**, **5**, **19**, **23**, **25**, and **26**), a direct coordination to calcium is still possible, however, with the consequence of shifting the cyclourea closer to the hydrophobic cage (Figure 4B). In addition to the above-described hydrophobic and metal interactions, all compounds are proposed to H-bond to either Phe26 and Gly28 main chain atoms or His46 side chain (Figure 4). The proposed binding mode recalls the experimentally determined X-ray structure of hGIIA sPLA2-bound indoxam derivatives (Figure 4C) for which a very similar coordination of calcium through a long chain carboxylate/phosphate moiety and a shorter amide substituent are also present. Aromatic substituents (phenyl, naphthyl) fill the previously described hydrophobic cage as for the herein described triazepandiones.<sup>40,41</sup>

The observed selectivity of triazepandiones for group V and X sPLA2s may be explained by the possible interaction of the triazepandione core with Leu-5 side chain, a residue specific to these two sPLA2 subtypes. Hence, group IB and IIA sPLA2s, for which no significant inhibitory activity could be detected for any of the herein described compounds, present a Phe-5 residue that would clash with the cyclourea in the currently proposed binding modes. It should be noticed that Phe-5 is precisely the residue demonstrated by X-ray diffraction studies<sup>40,41</sup> to explain the preferred binding of indoxam derivatives to groups IB and IIA sPLA2s (Figure 4C), by edge to face aromatic interactions with the indole ring of the synthetic inhibitors.<sup>42–44</sup>

The exact value of the *in silico* screen is unknown since it would require assaying both all predicted active and inactive targets, which is unfortunately not feasible and is the basic justification of a computer-guided target prioritization. We cannot exclude having selected sPLA2 for wrong reasons. However, the very stringent target selection procedure and the explanation of structure–activity relationships for triazepandione derivatives (Table 3, Figure 2) on the basis of predicted docking modes (Figure 4) render this hypothesis very unlikely. Random picking would produce a target rate for sPLA2 of 0.37% (eight copies out a total number of 2148 targets) while our *in silico* guidance selected sPLA2 because of much higher predicted target rates (25 and 13% for compounds **29** and **36**, respectively). Of course, the proposed target screening method is far from being perfect since it still generates more false positives than true positives as a classical ligand-based screening would do. There are in fact no reasons why a target-based screening should be much more accurate than a ligand-based screening provided that the screening engine is the same (molecular docking). Explanations for generating false positives in docking experiments are numerous.<sup>29,30</sup> Of particular concern here is the possible inaccurate modeling of protonation and tautomeric states which have been fixed for a particular entry but are known to be ligand-dependent.

The current screening of five compounds on a database of 2150 active sites is fast enough (total of 64 cpu-hours) to be applied to any orphan chemotype for which targets are to be discovered, or to identify additional targets (e.g. mediating putative side effects) for existing leads. Meanwhile, our collection of active sites has been updated<sup>24,31</sup> to reflect the current status of the PDB and now contains a total of 6415 druggable active sites. It is, however, still straightforward to screen, notably since molecular docking is easily amenable to parallelized data

distribution. However, due to the current target selection procedure based on enrichments in individual targets, proteins for which a single copy is present in our library are going to be missed. As predicting binding energies cannot be simply used to accurately rank complexes because of the known weakness of current fast scoring functions,<sup>45</sup> alternative ranking of targets (e.g. based on interaction fingerprint similarities<sup>46</sup>) or ligand efficiency<sup>47</sup> have to be developed to recover single-copy targets. One could also imagine enlarging the collection of available binding sites with 3-D models obtained by comparative modeling to X-ray templates.<sup>48</sup> Last, additional pockets calculated from either holo- or apo-enzymes<sup>23</sup> may open the possibility to search for allosteric regulators and not only for competitive inhibitors of ligands registered in the sc-PDB database.

## Conclusion

The 1,3,5-triazepan-2,6-dione scaffold is a novel contribution to the drug-like chemical space that combines two advantages: easy accessibility by parallel synthesis from the corresponding activated dipeptide precursors, and efficient distribution of five diversity points in a constrained pharmacophoric space. A first *in silico*-guided attempt to match this new chemical space with existing target space led us to identify human group V and X sPLA2s as targets for the new chemotype. Interestingly, these two sPLA2s and other members of this emerging family of enzymes have become attractive therapeutic targets in a number of inflammatory diseases including asthma, rheumatoid arthritis, atherosclerosis, and septic shock, as well as in different types of cancer.<sup>49–54</sup> Many different potent competitive inhibitors have been developed against the inflammatory-type human group IIA enzyme,<sup>51</sup> and some of these inhibitors or derivatives have been found to inhibit also human group V and X sPLA2s among other sPLA2s.<sup>41,55,56</sup> Although our current triazepandione compounds have modest affinities for sPLA2s, they appear to be selective for group V and X sPLA2s and thus are interesting lead compounds to develop in order to design more potent yet selective inhibitors of these particular sPLA2 subtypes that may be more important than group IIA sPLA2 in various human diseases.<sup>51,52,57,58</sup>

## Experimental Section

**Chemistry. General Procedures.** THF was distilled from Na/benzophenone. CH<sub>2</sub>Cl<sub>2</sub> and cyclohexane were distilled from CaH<sub>2</sub>. Thin-layer chromatography (TLC) was performed on silica gel 60 F254 (Merck) with detection by UV light and charring with 1% w/w ninhydrin in ethanol followed by heating. Flash column chromatography was carried out on silica gel (0.063–0.200 nm). HPLC analysis was performed on a Nucleosil C<sub>18</sub> column (5 μm, 3.9 × 150 mm) by using a linear gradient of A (0.1% TFA in H<sub>2</sub>O) and B (0.08% TFA in CH<sub>3</sub>CN) at a flow rate of 1.2 mL/min with UV detection at 214 nm. Optical rotations were recorded with a Perkin-Elmer polarimeter. IR spectra were recorded on a Perkin-Elmer Spectrum One in four scans with an ATR (attenuated total reflection) accessory. <sup>1</sup>H NMR and <sup>13</sup>C NMR spectra were recorded using Bruker Advance DPX-300, DPX-400, DPX-500 instruments. Mass spectra have been recorded using a MALDI-TOF apparatus (BRUKER Protein-TOF) and an ESI-TOF apparatus (Bruker microTOF).

**(6-Benzyl-1-methyl-4,7-dioxo-[1,3,5]triazepan-3-yl)-acetic Acid Methyl Ester (3).** Cyclo(Phe-gSar-CO) **1** (120 mg, 0.52 mmol) was dissolved in THF (6 mL) under Ar. Methyl bromoacetate (74 μL, 0.78 mmol) and KF/Al<sub>2</sub>O<sub>3</sub> 40 wt % (755 mg, 5.2 mmol) were then added, and the mixture was stirred 96 h at r.t. under inert atmosphere. Dilution in CH<sub>2</sub>Cl<sub>2</sub> and washing with H<sub>2</sub>O afforded the organic layer, which was dried over Na<sub>2</sub>SO<sub>4</sub> and evaporated. The crude residue was purified by flash column chromatography



with ethyl acetate as eluent to yield **3** (39 mg, 25%) as a white powder. C<sub>15</sub>H<sub>19</sub>N<sub>3</sub>O<sub>4</sub>, white solid, C<sub>18</sub>-RP-HPLC (A: 0.1% TFA in H<sub>2</sub>O, B: 0.08% TFA in MeCN, 0–100% B, 1.2 mL/min, 20 min): *t*<sub>R</sub> = 11.45 min; IR(solid):  $\nu_{\max}$  (cm<sup>-1</sup>) = 3286, 3182 (NH), 3027 (Csp<sup>2</sup>), 2922 (Csp<sup>3</sup>), 1750, 1681, 1638 (CO); <sup>1</sup>H NMR (300 MHz, CDCl<sub>3</sub>, 298 K):  $\delta$  = 2.81 (dd, *J* = 9, 14.4 Hz, CH<sub>2</sub>Ph, 1H), 3.13 (s, NCH<sub>3</sub>, 3H), 3.36 (dd, *J* = 4.5, 14.4 Hz, CH<sub>2</sub>Ph, 1H), 3.73 (s, OCH<sub>3</sub>, 3H), 4.01 (d, *J* = 17.8 Hz, NCH<sub>2</sub>, 1H), 4.17 (d, *J* = 15.7 Hz, NCH<sub>2</sub>N, 1H), 4.35 (d, *J* = 17.8 Hz, NCH<sub>2</sub>, 1H), 4.58–4.64 (m, NCHCO, 1H), 4.65 (br., NH), 5.45 (d, *J* = 15.7 Hz, NCH<sub>2</sub>N, 1H), 7.27–7.36 (m, H-Ar, 5H); HRMS(ESI): *m/z*: calculated for C<sub>15</sub>H<sub>20</sub>N<sub>3</sub>O<sub>4</sub>: 306.1448, found: 306.1436.

**7-Benzyl-3-(2-hydroxy-ethyl)-5-methyl-[1,3,5]triazepan-2,6-dione (6)**. Acid **5** (410 mg, 1.41 mmol) was dissolved in THF (20 mL) under inert atmosphere, and NMM (186  $\mu$ L, 1.69 mmol) was added. The solution was cooled to -20 °C, and *i*BuOCOCl (222  $\mu$ L, 1.69 mmol) was added. The reaction mixture was stirred 25 min at -20 °C. Salts were quickly filtered at room temperature, and the mixture was replaced in the -20 °C bath. A solution of NaBH<sub>4</sub> (160 mg, 4.23 mmol) in H<sub>2</sub>O (5 mL) was added. After 20 min at -20 °C, the mixture was allowed to warm to room temperature. Dilution in ethyl acetate was followed by a workup with brine. The organic layer was dried over Na<sub>2</sub>SO<sub>4</sub> and evaporated. The crude residue was purified by silica gel column chromatography (CH<sub>2</sub>-Cl<sub>2</sub>/MeOH/AcOH 95:5:1, v/v/v) to afford **6** (196 mg, 50%) as a white powder. C<sub>14</sub>H<sub>19</sub>N<sub>3</sub>O<sub>3</sub>, C<sub>18</sub>-RP-HPLC (A: 0.1% TFA in H<sub>2</sub>O, B: 0.08% TFA in MeCN, 0–100% B, 1.2 mL/min, 20 min): *t*<sub>R</sub> = 13.34 min; IR(solid):  $\nu_{\max}$  (cm<sup>-1</sup>) = 3397 (NH), 3279 (OH), 3023 (Csp<sup>2</sup>), 2918 (Csp<sup>3</sup>), 1644, 1620 (CO); <sup>1</sup>H NMR (300 MHz, CDCl<sub>3</sub>, 298 K):  $\delta$  = 2.96 (dd, *J* = 8.3, 14.3 Hz, CH<sub>2</sub>Ph, 1H), 3.23 (s, NCH<sub>3</sub>, 3H), 3.42–3.53 (m, CH<sub>2</sub>Ph, NCH<sub>2</sub>CH<sub>2</sub>, 2H), 3.71–3.81 (m., NCH<sub>2</sub>CH<sub>2</sub>, HOCH<sub>2</sub>CH<sub>2</sub>, 3H), 4.42 (d, *J* = 15.7 Hz, NCHN, 1H), 4.70–4.75 (m, NCHCO, 1H), 5.40–5.45 (m, NCHN, 2H), 7.38–7.48 (m, CH-Ar, 5H); <sup>13</sup>C NMR (75 MHz, CDCl<sub>3</sub>, 298 K):  $\delta$  = 30.40 (CH<sub>3</sub>), 33.94, 48.01 (CH<sub>2</sub>), 52.08 (CH), 57.64, 58.91 (CH<sub>2</sub>), 123.11, 124.80, 124.98, 125.41 (CH-Ar), 132.60 (Cq-Ar), 154.38, 166.10 (CO); HRMS(ESI): *m/z*: calculated for C<sub>14</sub>H<sub>20</sub>N<sub>3</sub>O<sub>3</sub>: 278.1499, found: 278.1475.

**4-(6-Benzyl-1-methyl-4,7-dioxo-[1,3,5]triazepan-3-yl)-but-2-enoic Acid *tert*-Butyl Ester (8)**. Under inert atmosphere, CH<sub>2</sub>Cl<sub>2</sub> (0.5 mL) was introduced in a flask. Oxalyl chloride (57  $\mu$ L, 0.65 mmol) was added via a hypodermic syringe, and the mixture was cooled to -20 °C. DMSO (91  $\mu$ L, 1.29 mmol) was added, and the mixture was stirred at -20 °C for 10 min. A solution of alcohol **6** (120 mg, 0.43 mmol) in CH<sub>2</sub>Cl<sub>2</sub> (1.5 mL) was added dropwise, and the mixture was stirred at -20 °C for an additional 20 min. DIPEA (450  $\mu$ L, 2.6 mmol) was then added. After 5 min at -20 °C, the mixture was allowed to warm to room temperature. H<sub>2</sub>O (10 mL) was added, and the system was stirred at r.t. for 10 min. Extraction with CH<sub>2</sub>Cl<sub>2</sub> (4  $\times$  25 mL) provided the organic layer which was washed with KHSO<sub>4</sub> 1 N and brine. The organic layer was dried over Na<sub>2</sub>SO<sub>4</sub> and evaporated to give the aldehyde **7**. Formation of **7** was followed by TLC, and the compound was directly used in the next step. (Ph)<sub>3</sub>P=CHCOO*t*Bu (244 mg, 0.65 mmol) was added to a solution of **7** in CH<sub>2</sub>Cl<sub>2</sub> under inert atmosphere, and the reaction mixture was stirred at room temperature for 2.5 h. The reaction was quenched by addition of water. After separation, the organic layer was dried over Na<sub>2</sub>SO<sub>4</sub> and evaporated. The crude residue was purified by flash column chromatography (AcOEt/cyclohexane/AcOH, 1:1:0.1 v/v/v) to afford *Z*-**8** (18.6 mg, 11.6%) as a white powder and *E*-**8** contaminated by (Ph)<sub>3</sub>PO. *E*-**8** was isolated after selective precipitation of (Ph)<sub>3</sub>PO in Et<sub>2</sub>O and subsequent filtration. Evaporation of solvent yielded pure *E*-**8** (93.5 mg, 58.2%) as a white powder. Global yield of the reaction was calculated: 70%, *Z/E* ratio: 1/6. C<sub>20</sub>H<sub>27</sub>N<sub>3</sub>O<sub>4</sub>, *Z* isomer: C<sub>18</sub>-RP-HPLC (A: 0.1% TFA in H<sub>2</sub>O, B: 0.08% TFA in MeCN, 0–100% B, 1.2 mL/min, 20 min): *t*<sub>R</sub> = 15.85 min; IR-(solid):  $\nu_{\max}$  (cm<sup>-1</sup>) = 3281, 3211 (NH), 3070 (Csp<sup>2</sup>), 2919, 2851 (Csp<sup>3</sup>), 1705, 1683, 1645 (CO); <sup>1</sup>H NMR (300 MHz, CDCl<sub>3</sub>, 298 K):  $\delta$  = 1.46 (s, (CH<sub>3</sub>)<sub>3</sub>, 9H), 2.80 (dd, *J* = 9.3, 14.4 Hz, CH<sub>2</sub>Ph, 1H), 3.09 (s, NCH<sub>3</sub>, 3H), 3.35 (dd, *J* = 4.5, 14.4 Hz, CH<sub>2</sub>Ph, 1H),

4.36 (d, *J* = 15.6 Hz, NCHN, 1H), 4.45 (br., NH), 4.53–4.59 (m, NCH<sub>2</sub>CH, NCHCO, 3H), 5.24 (d, *J* = 15.6 Hz, NCHN, 1H), 5.83–5.87 (m, CHCHCO, 1H), 6.12 (td, *J* = 7.1, 11.4 Hz, CH<sub>2</sub>CHCH, 1H), 7.24–7.36 (m, CH-Ar, 5H); <sup>13</sup>C NMR (75 MHz, CDCl<sub>3</sub>, 298 K):  $\delta$  = 28.14, 34.28 (CH<sub>3</sub>), 38.43, 45.86 (CH<sub>2</sub>), 56.27 (CH), 61.53 (CH<sub>2</sub>), 81.09 (Cq), 123.98 (CH), 127.31, 129.00, 129.31 (CH-Ar), 136.18 (Cq-Ar), 143.12 (CH), 157.20, 169.89, 189.05 (CO); HRMS (ESI): *m/z*: calculated for C<sub>20</sub>H<sub>28</sub>N<sub>3</sub>O<sub>4</sub>: 374.2074, found: 374.2069. *E* isomer: C<sub>18</sub>-RP-HPLC (A: 0.1% TFA in H<sub>2</sub>O, B: 0.08% TFA in MeCN, 0–100% B, 1.2 mL/min, 20 min): *t*<sub>R</sub> = 15.18 min; <sup>1</sup>H NMR (300 MHz, CDCl<sub>3</sub>, 298 K):  $\delta$  = 1.46 (s, (CH<sub>3</sub>)<sub>3</sub>, 9H), 2.80 (dd, *J* = 9.0, 14.4 Hz, CH<sub>2</sub>Ph, 1H), 3.07 (s, NCH<sub>3</sub>, 3H), 3.35 (dd, *J* = 4.8, 14.4 Hz, CH<sub>2</sub>Ph, 1H), 4.36 (d, *J* = 15.6 Hz, NCHN, 1H), 4.13–4.17 (m, NCH<sub>2</sub>CH, 2H), 4.55–4.60 (m, NCHCO, 1H), 4.75 (d, *J* = 1.8 Hz, NH, 1H), 5.24 (d, *J* = 15.6 Hz, NCHN, 1H), 5.82 (td, *J* = 1.4, 15.7 Hz, CHCHCO, 1H), 6.71 (td, *J* = 5.4, 15.9 Hz, CH<sub>2</sub>CHCH, 1H), 7.25–7.34 (m, CH-Ar, 5H); <sup>13</sup>C NMR (75 MHz, CDCl<sub>3</sub>, 298 K):  $\delta$  = 28.08, 34.60 (CH<sub>3</sub>), 38.27, 43.38 (CH<sub>2</sub>), 56.27 (CH), 61.31 (CH<sub>2</sub>), 80.89 (Cq), 125.05 (CH), 127.31, 128.98, 129.35 (CH-Ar), 136.15 (Cq-Ar), 143.69 (CH), 157.09, 164.89, 169.83 (CO); HRMS (ESI): *m/z*: calculated for C<sub>20</sub>H<sub>28</sub>N<sub>3</sub>O<sub>4</sub>: 374.2074, found: 374.2071.

**4-(6-Benzyl-1-methyl-4,7-dioxo-[1,3,5]triazepan-3-yl)-butyric Acid *tert*-Butyl Ester (9)**. **8** (110 mg, 0.29 mmol) was dissolved in EtOH (20 mL). Pd/C 10wt % (20 mg) was added. The system was stirred for 16 h under hydrogen atmosphere. Filtration over Celite yielded **9** (105 mg, 97%) as a white powder. C<sub>20</sub>H<sub>29</sub>N<sub>3</sub>O<sub>4</sub>, C<sub>18</sub>-RP-HPLC (A: 0.1% TFA in H<sub>2</sub>O, B: 0.08% TFA in MeCN, 0–100% B, 1.2 mL/min, 20 min): *t*<sub>R</sub> = 15.33 min; IR(solid):  $\nu_{\max}$  (cm<sup>-1</sup>) = 3270, 3020 (NH), 3066 (Csp<sup>2</sup>), 2973, 2934 (Csp<sup>3</sup>), 1722, 1711, 1686, 1674, 1646, 1630 (CO); <sup>1</sup>H NMR (300 MHz, CDCl<sub>3</sub>, 298 K):  $\delta$  = 1.42 (s, (CH<sub>3</sub>)<sub>3</sub>, 9H), 1.77–1.82 (m, NCH<sub>2</sub>CH<sub>2</sub>, 2H), 2.21–2.26 (m, COCH<sub>2</sub>CH<sub>2</sub>, 2H), 2.78 (dd, *J* = 9.3, 14.3 Hz, CH<sub>2</sub>-Ph, 1H), 3.13 (s, NCH<sub>3</sub>, 3H), 3.31–3.37 (m, CH<sub>2</sub>Ph, NCH<sub>2</sub>CH<sub>2</sub>, 2H), 3.42–3.47 (m, NCH<sub>2</sub>CH<sub>2</sub>, 1H), 4.25 (d, *J* = 15.6 Hz, NCH<sub>2</sub>N, 1H), 4.40 (br., NH), 4.51–4.56 (m, NCHCO, 1H), 5.23 (d, *J* = 15.6 Hz, NCH<sub>2</sub>N, 1H), 7.24–7.32 (m, CH-Ar, 5H); <sup>13</sup>C NMR (75 MHz, CDCl<sub>3</sub>, 298 K):  $\delta$  = 24.38 (CH<sub>2</sub>), 28.07 (CH<sub>3</sub>), 32.23 (CH<sub>2</sub>), 34.52 (CH<sub>3</sub>), 38.56, 48.25 (CH<sub>2</sub>), 56.47 (CH), 61.85 (CH<sub>2</sub>), 80.55 (Cq), 127.28, 128.98, 129.32 (CH-Ar), 156.48, 169.89, 172.51 (CO); HRMS (ESI): *m/z*: calculated for C<sub>20</sub>H<sub>30</sub>N<sub>3</sub>O<sub>4</sub>: 376.2231, found: 376.2210.

**4-(6-Benzyl-1-methyl-4,7-dioxo-[1,3,5]triazepan-3-yl)-butyric Acid (10)**. **9** (48 mg, 0.13 mmol) was dissolved in TFA/CH<sub>2</sub>Cl<sub>2</sub> (1:1, v/v), (1 mL), and the reaction was stirred at room temperature for 30 min. Solvents were evaporated and afforded **10** (22 mg, 55%) as a white powder. C<sub>16</sub>H<sub>21</sub>N<sub>3</sub>O<sub>4</sub>, C<sub>18</sub>-RP-HPLC (A: 0.1% TFA in H<sub>2</sub>O, B: 0.08% TFA in MeCN, 0–100% B, 1.2 mL/min, 20 min): *t*<sub>R</sub> = 11.52 min; IR(solid):  $\nu_{\max}$  (cm<sup>-1</sup>) = 3301 (OH), 2946, 2923, 2853 (Csp<sup>3</sup>), 1686, 1613 (CO); HRMS (ESI): *m/z*: calculated for C<sub>16</sub>H<sub>22</sub>N<sub>3</sub>O<sub>4</sub>: 320.1605, found: 320.1618.

**4-(6-Benzyl-1-methyl-4,7-dioxo-[1,3,5]triazepan-3-yl)-butyramide (11)**. Sieber resin (0.084 mmol) was swollen in DMF and rinsed twice prior to use. Removal of the Fmoc group was achieved by treatment with a mixture of DMF/piperidine (1:1, v/v) (1 mL) for 20 min (repeated twice), followed by washings with DMF ( $\times$ 6). A solution of **10** (18 mg, 0.056 mmol), BOP (26 mg, 0.059 mmol), and HOBt (8 mg, 0.059 mmol) dissolved in DMF was prepared and added onto the resin. DIPEA (30  $\mu$ L, 0.17 mmol) was then added, and the mixture was stirred at room temperature for 1.5 h. The resin was filtered, washed with DMF ( $\times$ 4) and CH<sub>2</sub>Cl<sub>2</sub> ( $\times$ 4) and dried under high vacuum. Cleavage by treatment with TFA/CH<sub>2</sub>Cl<sub>2</sub> (1:9, v/v) (1 mL) was performed at room temperature in 40 min. The filtrate was collected, and the resin was washed with CH<sub>2</sub>Cl<sub>2</sub>. The solvents were evaporated. The crude residue was purified by flash column chromatography (CHCl<sub>3</sub>/MeOH 10:1, v/v) to afford **11** (12 mg, 68%) as a white powder. C<sub>16</sub>H<sub>22</sub>N<sub>4</sub>O<sub>3</sub>, C<sub>18</sub>-RP-HPLC (A: 0.1% TFA in H<sub>2</sub>O, B: 0.08% TFA in MeCN, 0–100% B, 1.2 mL/min, 20 min): *t*<sub>R</sub> = 9.55 min; IR(solid):  $\nu_{\max}$  (cm<sup>-1</sup>) = 3334 (NH), 2934 (Csp<sup>3</sup>), 1630 (CO); <sup>1</sup>H NMR (300 MHz, CDCl<sub>3</sub>, 298 K):  $\delta$  = 1.82–1.89 (m, NCH<sub>2</sub>CH<sub>2</sub>, 2H), 2.19–2.24



(m, CH<sub>2</sub>CH<sub>2</sub>CO, 2H), 2.79 (dd, *J* = 9.0, 14.5 Hz, CH<sub>2</sub>Ph, 1H), 3.13 (s, NCH<sub>3</sub>, 3H), 3.32–3.41 (m, CH<sub>2</sub>Ph, NCH<sub>2</sub>CH<sub>2</sub>, 2H), 3.51–3.58 (NCH<sub>2</sub>CH<sub>2</sub>, 1H), 4.19 (d, *J* = 15.7 Hz, NCH<sub>2</sub>N, 1H), 4.54–4.59 (m, NCHCO, NH, 2H), 5.26 (d, *J* = 15.7 Hz, NCH<sub>2</sub>N, 1H), 5.38 (br., NH<sub>2</sub>, 1H), 6.29 (br., NH<sub>2</sub>, 1H), 7.24–7.37 (m, CH-Ar, 5H); <sup>13</sup>C NMR (75 MHz, CDCl<sub>3</sub>, 298 K): δ = 24.76, 32.13 (CH<sub>2</sub>), 34.59 (CH<sub>3</sub>), 39.20, 47.98 (CH<sub>2</sub>), 56.10 (CH), 61.64 (CH<sub>2</sub>), 127.34, 129.01, 129.31 (Cq-Ar), 136.19 (Cq-Ar), 157.93, 169.87, 174.94 (CO); HRMS (ESI): *m/z*: calculated for C<sub>16</sub>H<sub>23</sub>N<sub>4</sub>O<sub>3</sub>: 319.1765, found: 319.1768.

**2-(6-Benzyl-1-methyl-4,7-dioxo-[1,3,5]triazepan-3-yl)-acetamide (12).** **12** was obtained from **5** according to the procedure described for **11** in 74% yield. C<sub>14</sub>H<sub>18</sub>N<sub>4</sub>O<sub>3</sub>, C<sub>18</sub>-RP-HPLC (A: 0.1% TFA in H<sub>2</sub>O, B: 0.08% TFA in MeCN, 0–100% B, 1.2 mL/min, 20 min): *t*<sub>R</sub> = 9.00 min; IR(solid): ν<sub>max</sub> (cm<sup>-1</sup>) = 3287 (NH), 1635 (CO); HRMS (ESI): *m/z*: calculated for C<sub>14</sub>H<sub>19</sub>N<sub>4</sub>O<sub>3</sub>: 291.1452, found: 291.1456.

**4-(6-Benzyl-1-methyl-4,7-dioxo-[1,3,5]triazepan-3-yl)-but-2-enoic Acid (*E* isomer) (13).** **13** was obtained from **8** (*E* isomer) according to the method described for the preparation of **10** in 54% yield. C<sub>16</sub>H<sub>19</sub>N<sub>3</sub>O<sub>4</sub>, C<sub>18</sub>-RP-HPLC (A: 0.1% TFA in H<sub>2</sub>O, B: 0.08% TFA in MeCN, 0–100% B, 1.2 mL/min, 20 min): *t*<sub>R</sub> = 11.42 min; IR(solid): ν<sub>max</sub> (cm<sup>-1</sup>) = 3279 (OH), 2924 (Csp<sup>3</sup>), 1698, 1661, 1607 (CO); <sup>1</sup>H NMR (300 MHz, CDCl<sub>3</sub>, 298 K): δ = 2.78 (dd, *J* = 6.5, 14.1 Hz, CH<sub>2</sub>Ph, 1H), 2.90 (s, NCH<sub>3</sub>, 3H), 3.05 (dd, *J* = 6.9, 14.1 Hz, CH<sub>2</sub>Ph, 1H), 4.07–4.12 (m, NCH<sub>2</sub>CH, 2H), 4.24 (d, *J* = 15.8 Hz, NCH<sub>2</sub>N, 1H), 4.80–4.86 (m, NCHCO, 1H), 5.58 (d, *J* = 15.8 Hz, NCH<sub>2</sub>N, 1H), 5.80 (d, *J* = 15.7 Hz, CHCHCO, 1H), 6.30 (d, *J* = 3.2 Hz, NN, 1H), 6.70 (td, *J* = 4.9, 15.7 Hz, NCH<sub>2</sub>CH, 1H), 7.16–7.34 (m, CH-Ar, 5H); <sup>13</sup>C NMR (75 MHz, CDCl<sub>3</sub>, 298 K): δ = 33.85 (CH), 36.62 (CH<sub>2</sub>), 49.51 (CH<sub>2</sub>), 54.50 (CH), 61.29 (CH<sub>2</sub>), 122.49 (CH), 126.66, 128.52, 129.88 (CH-Ar), 138.51 (Cq-Ar), 145.12 (CH), 156.49, 167.32, 171.10 (CO); HRMS (ESI): *m/z*: calculated for C<sub>16</sub>H<sub>20</sub>N<sub>3</sub>O<sub>4</sub>: 318.1448, found: 318.1433.

**(1-Methyl-6-naphthalen-2-ylmethyl-4,7-dioxo-[1,3,5]triazepan-3-yl)-acetic Acid *tert*-Butyl Ester (23).** **23** was obtained from **22** according to the method described for the preparation of **3** in 38% yield. C<sub>22</sub>H<sub>27</sub>N<sub>3</sub>O<sub>4</sub>, white solid, C<sub>18</sub>-RP-HPLC (A: 0.1% TFA in H<sub>2</sub>O, B: 0.08% TFA in MeCN, 0–100% B, 1.2 mL/min, 20 min): *t*<sub>R</sub> = 19.02 min; IR(solid): ν<sub>max</sub> (cm<sup>-1</sup>) = 3286, 3208 (NH), 2923, 2852 (Csp<sup>3</sup>), 1737, 1655 (CO); <sup>1</sup>H NMR (300 MHz, CDCl<sub>3</sub>, 298 K): δ = 1.44 (s, (CH<sub>3</sub>)<sub>3</sub>, 3H), 2.97 (dd, *J* = 9.1, 14.2 Hz, CH<sub>2</sub>Ph, 1H), 3.14 (s, NCH<sub>3</sub>, 3H), 3.52 (dd, *J* = 4.7, 14.2 Hz, CH<sub>2</sub>Ph, 1H), 3.85 (d, *J* = 17.7 Hz, NCH<sub>2</sub>CO, 1H), 4.16 (d, *J* = 15.7 Hz, NCH<sub>2</sub>N, 1H), 4.27 (d, *J* = 17.7 Hz, NCH<sub>2</sub>CO, 1H), 4.60 (br., NH), 4.68–4.72 (m, NCHCO, 1H), 5.46 (, *J* = 15.7 Hz, NCH<sub>2</sub>N, 1H), 7.35–7.49 (m, CH-Ar, 3H), 7.73–7.83 (m, CH-Ar, 4H); <sup>13</sup>C NMR (75 MHz, CDCl<sub>3</sub>, 298 K): δ = 28.04, 34.68 (CH<sub>3</sub>), 38.44, 51.47 (CH<sub>2</sub>), 55.80 (CH), 62.84 (CH<sub>2</sub>), 82.30 (Cq), 125.94, 126.38, 126.93, 127.64, 128.34, 128.84 (CH-Ar), 132.56, 133.49, 133.54 (Cq-Ar), 157.66, 168.93, 169.84 (CO); HRMS(ESI): *m/z*: calculated for C<sub>22</sub>H<sub>28</sub>N<sub>3</sub>O<sub>4</sub>: 396.2074; found: 396.2082.

**(5-Naphthalen-2-ylmethyl-4,7-dioxo-octahydro-3a,6,8-triazazulen-8-yl)-acetic Acid *tert*-Butyl Ester (34).** **34** was obtained from **30** according to the method described for the preparation of **3** in 29% yield. C<sub>24</sub>H<sub>29</sub>N<sub>3</sub>O<sub>4</sub>, white solid, C<sub>18</sub>-RP-HPLC (A: 0.1% TFA in H<sub>2</sub>O, B: 0.08% TFA in MeCN, 0–100% B, 1.2 mL/min, 20 min): *t*<sub>R</sub> = 15.29 min; IR(solid): ν<sub>max</sub> (cm<sup>-1</sup>) = 3275, 3203 (NH), 3061 (Csp<sup>2</sup>), 2975, 2925 (Csp<sup>3</sup>), 1740, 1673, 1650 (CO); <sup>1</sup>H NMR (300 MHz, CDCl<sub>3</sub>, 298 K): δ = 1.44 (s, CH<sub>3</sub>, 9H), 1.88–2.19 (m, CH<sub>2</sub>, 4H), 2.93–3.01 (m, CH<sub>2</sub>Nal, 1H), 3.56–3.68 (m, CH<sub>2</sub>Nal, NCH<sub>2</sub>CH<sub>2</sub>, 3H), 3.74 (d, *J* = 18.1 Hz, NCH<sub>2</sub>CO, 1H), 4.42 (d, *J* = 18.1 Hz, NCH<sub>2</sub>CO, 1H), 4.73 (d, *J* = 2.1 Hz, NH), 5.78 (m, NCHN, 1H), 7.39–7.45 (m, H-Ar, 3H), 7.77–7.82 (m, H-Ar, 4H); <sup>13</sup>C NMR (75 MHz, CDCl<sub>3</sub>, 298 K): δ = 22.36 (CH<sub>2</sub>), 28.03 (CH<sub>3</sub>), 29.69, 30.86, 38.64, 45.57, 46.08 (CH<sub>2</sub>), 57.44, 68.65 (CH), 2.12 (Cq), 125.83, 126.25, 126.23, 127.61, 127.68, 128.47, 128.68 (CH-Ar), 132.49, 133.52, 134.09 (Cq-Ar), 159.45, 168.07, 169.41 (CO); HRMS(ESI): *m/z*: calculated for C<sub>24</sub>H<sub>30</sub>N<sub>3</sub>O<sub>4</sub>: 424.2231, found: 424.2220.

**Virtual Screening of the sc-PDB Database.** A subset of the Protein DataBank<sup>21</sup> comprising 2148 well-characterized binding sites (release 1.0 of the sc-PDB)<sup>20</sup> was screened to identify putative targets for 5 compounds (**1**, **5**, **16**, **29**, **36**; Tables 1–3) representative of physically available triazepandiones. Automated input data preparation for the GOLD 2.1 docking program<sup>59</sup> was achieved using an in-house perl script as previously described.<sup>20</sup> For each entry of the sc-PDB database, initial PDB coordinates of the protein were converted to TRIPOS mol2 format<sup>60</sup> while adding all hydrogen atoms, using the SYBYL 6.91 package.<sup>60</sup> Ligands were built in SYBYL starting from the X-ray structure of the 1,3,5-triazepan-2,6-dione **2**.<sup>32</sup> Compounds were ionized manually at their most likely ionization state at pH 7.4 and further minimized using 100 steps of steepest descent minimization using the TRIPOS force field and finally saved as 3-D mol2 files. A GOLD configuration file (gold\_auto) was defined for each sc-PDB entry, including the absolute path of the corresponding protein mol2 file and the 3-D coordinates of the active site center deduced from the coordinates of the cognate ligand. Fast virtual screening settings were chosen for launching a separate job per entry. Fifteen independent jobs were submitted, and the average fitness score for each PDB entry was saved in an ASCII file. In the current study, 32 processors of a SGI Origin3800 supercomputer were used to screen the full database in ca. 2 h (total of 64 cpu-hours).

**Preparation of Recombinant Human sPLA2s.** Recombinant hGIB, hGIIA, hGV, and hGX sPLA2s were produced in *E. coli* as described previously.<sup>55</sup> Recombinant hGIII sPLA2 catalytic domain was produced in *Drosophila* S2 insect cells as previously described for human group IID sPLA2.<sup>55</sup> The detailed protocol will be described elsewhere.

**sPLA2 Assays for Inhibition Analysis.** sPLA2 assays were performed using radiolabeled *E. coli* membranes as substrate as described.<sup>39,55</sup> Assays were carried in a final volume of 300 μL. The binding buffer was 100 mM Tris, pH 8.0, 10 mM CaCl<sub>2</sub>, 0.1% bovine serum albumin. In these assays, the inhibitors were first preincubated with sPLA2s for 10 min in 100 μL of binding buffer. Two hundred milliliters of *E. coli* substrate (containing 100,000 dpm of <sup>3</sup>H-oleate labeled phospholipids) diluted in binding buffer was then added, and the reaction was continued for 15 min at room temperature. sPLA2 activity was stopped by addition of 300 μL of a solution containing 0.1 M EDTA, pH 8.0, and 1% free fatty acid bovine serum albumin. After centrifugation at 14000g for 3 min, supernatants containing the hydrolyzed phospholipids were collected and counted. The concentrations of human sPLA2s were adjusted to ensure hydrolysis rates within the linear range of enzymatic assays. Results are expressed as percentage of residual inhibition of sPLA2 activity at the indicated concentration of inhibitors or as IC<sub>50</sub> values. IC<sub>50</sub> value is defined as the concentration of inhibitor that decreases the sPLA2 specific activity to 50%.

**Acknowledgment.** This work is supported by grants from the French Ministry of Research and Technology (to P.M.), the Association pour la Recherche sur le Cancer (to S.B. and G. L.), the Canadian Institutes of Health Research in partnership with the Arthritis Society (to E.B.), Région Alsace and ImmuPharma France. CIFRE fellowship from ImmuPharma France and the Association Nationale pour la Recherche Technique (ANRT) for G. Léna. is gratefully acknowledged. We wish to thank the Centre Informatique National de l'Enseignement Supérieur (CINES, Montpellier, France) for the generous allocation of computing time on the SGI3800 supercomputer, and Prof. M. Gelb for helpful discussions. Last, we sincerely thank the research groups of Dr. Michael Coughtrie (University of Dundee, U.K.), Prof. Céline Tarnus (Ecole Nationale Supérieure de Chimie, Mulhouse, France), Prof. Elizabeth Sarciron (Faculté de Pharmacie, Lyon, France), Prof. Vern Schramm (Albert Einstein School of Medicine, New York, NY), and Prof. Leonardo Scapozza (ETH Zürich, Switzerland) for the biological evaluation of a few compounds on selected targets (estrogen

sulfotransferase, methionine aminopeptidase, purine nucleoside phosphorylase, thymidine kinase).

## References

- Lindsay, M. A. Target discovery. *Nat. Rev. Drug Discovery* **2003**, *2*, 831–838.
- Bleicher, K. H.; Bohm, H. J.; Muller, K.; Alanine, A. I. Hit and lead generation: beyond high-throughput screening. *Nat. Rev. Drug Discovery* **2003**, *2*, 369–378.
- Eggert, U. S.; Kiger, A. A.; Richter, C.; Perlman, Z. E.; Perrimon, N.; Mitchison, T. J.; Field, C. M. Parallel Chemical Genetic and Genome-Wide RNAi Screens Identify Cytokinesis Inhibitors and Targets. *PLoS Biol.* **2004**, *2*, e379.
- Edwards, B. S.; Oprea, T.; Prossnitz, E. R.; Sklar, L. A. Flow cytometry for high-throughput, high-content screening. *Curr. Opin. Chem. Biol.* **2004**, *8*, 392–398.
- Kwok, T. C.; Ricker, N.; Fraser, R.; Chan, A. W.; Burns, A.; Stanley, E. F.; McCourt, P.; Cutler, S. R.; Roy, P. A small-molecule screen in *C. elegans* yields a new calcium channel antagonist. *Nature* **2006**, *441*, 91–95.
- Kubinyi, H. Chance favors the prepared mind—from serendipity to rational drug design. *J. Recept. Signal Transduct. Res.* **1999**, *19*, 15–39.
- Hoffman, B. T.; Nelson, M. R.; Burdick, K.; Baxter, S. M. Protein tyrosine phosphatases: strategies for distinguishing proteins in a family containing multiple drug targets and anti-targets. *Curr. Pharm. Des.* **2004**, *10*, 1161–1181.
- Leach, A. R.; Hann, M. M. The in silico world of virtual libraries. *Drug Discovery Today* **2000**, *5*, 326–336.
- Parsons, A. B.; Geyer, R.; Hughes, T. R.; Boone, C. Yeast genomics and proteomics in drug discovery and target validation. *Prog. Cell Cycle Res.* **2003**, *5*, 159–166.
- Hopkins, A. L.; Groom, C. R. The druggable genome. *Nat. Rev. Drug Discovery* **2002**, *1*, 727–730.
- Kauvar, L. M.; Higgins, D. L.; Villar, H. O.; Sportsman, J. R.; Engqvist-Goldstein, A.; Bukar, R.; Bauer, K. E.; Dilley, H.; Rocke, D. M. Predicting ligand binding to proteins by affinity fingerprinting. *Chem. Biol.* **1995**, *2*, 107–118.
- Dixon, S. L.; Villar, H. O. Bioactive diversity and screening library selection via affinity fingerprinting. *J. Chem. Inf. Comput. Sci.* **1998**, *38*, 1192–1203.
- Lessel, U. F.; Briem, H. Flexsim-X: a method for the detection of molecules with similar biological activity. *J. Chem. Inf. Comput. Sci.* **2000**, *40*, 246–253.
- Bock, J. R.; Gough, D. A. Virtual screen for ligands of orphan G protein-coupled receptors. *J. Chem. Inf. Model.* **2005**, *45*, 1402–1414.
- Oloff, S.; Zhang, S.; Sukumar, N.; Breneman, C.; Tropsha, A. Chemometric Analysis of Ligand Receptor Complementarity: Identifying Complementary Ligands Based on Receptor Information (CoLiBRI). *J. Chem. Inf. Model.* **2006**, *46*, 844–851.
- Lamb, M. L.; Burdick, K. W.; Toba, S.; Young, M. M.; Skillman, A. G.; Zou, X.; Arnold, J. R.; Kuntz, I. D. Design, docking, and evaluation of multiple libraries against multiple targets. *Proteins* **2001**, *42*, 296–318.
- Fernandes, M. X.; Kairys, V.; Gilson, M. K. Comparing ligand interactions with multiple receptors via serial docking. *J. Chem. Inf. Comput. Sci.* **2004**, *44*, 1961–1970.
- Chen, Y. Z.; Ung, C. Y. Prediction of potential toxicity and side effect protein targets of a small molecule by a ligand-protein inverse docking approach. *J. Mol. Graph. Model.* **2001**, *20*, 199–218.
- Chen, Y. Z.; Zhi, D. G. Ligand-protein inverse docking and its potential use in the computer search of protein targets of a small molecule. *Proteins* **2001**, *43*, 217–226.
- Paul, N.; Kellenberger, E.; Bret, G.; Muller, P.; Rognan, D. Recovering the true targets of specific ligands by virtual screening of the protein data bank. *Proteins* **2004**, *54*, 671–680.
- Berman, H. M.; Westbrook, J.; Feng, Z.; Gilliland, G.; Bhat, T. N.; Weissig, H.; Shindyalov, I. N.; Bourne, P. E. The Protein Data Bank. *Nucleic Acids Res.* **2000**, *28*, 235–242.
- Hendlich, M.; Rippmann, F.; Barnickel, G. LIGSITE: automatic and efficient detection of potential small molecule-binding sites in proteins. *J. Mol. Graph. Model.* **1997**, *15*, 359–363, 389.
- An, J.; Totrov, M.; Abagyan, R. Pocketome via comprehensive identification and classification of ligand binding envelopes. *Mol. Cell. Proteomics* **2005**, *4*, 752–761.
- Kellenberger, E.; Muller, P.; Schalon, C.; Bret, G.; Foata, N.; Rognan, D. sc-PDB: an Annotated Database of Druggable Binding Sites from the Protein Data Bank. *J. Chem. Inf. Model.* **2006**, *46*, 717–727.
- Gold, N. D.; Jackson, R. M. A searchable database for comparing protein–ligand binding sites for the analysis of structure–function relationships. *J. Chem. Inf. Model.* **2006**, *46*, 736–742.
- Hu, L.; Benson, M. L.; Smith, R. D.; Lerner, M. G.; Carlson, H. A. Binding MOAD (Mother Of All Databases). *Proteins* **2005**, *60*, 333–340.
- Schmitt, S.; Kuhn, D.; Klebe, G. A new method to detect related function among proteins independent of sequence and fold homology. *J. Mol. Biol.* **2002**, *323*, 387–406.
- Gold, N. D.; Jackson, R. M. SitesBase: a database for structure-based protein–ligand binding site comparisons. *Nucleic Acids Res.* **2006**, *34*, D231–234.
- Verdonk, M. L.; Cole, J. C.; Hartshorn, M. J.; Murray, C. W.; Taylor, R. D. Improved protein–ligand docking using GOLD. *Proteins* **2003**, *52*, 609–623.
- Kellenberger, E.; Rodrigo, J.; Muller, P.; Rognan, D. Comparative evaluation of eight docking tools for docking and virtual screening accuracy. *Proteins* **2004**, *57*, 225–242.
- The sc-PDB database is available at <http://bioinfo-pharma.u-strasbg.fr/sc-PDB>.
- Lena, G.; Lallemand, E.; Gruner, A. C.; Boeglin, J.; Roussel, S.; Schaffner, A. P.; Aubry, A.; Franetich, J. F.; Mazier, D.; Landau, I.; Briand, J. P.; Didierjean, C.; Rénia, L.; Guichard, G. 1,3,5-Triazepan-2,6-diones as Structurally Diverse and Conformationally Constrained Dipeptide Mimetics. Identification of Malaria Liver Stage Inhibitors From a Small Pilot Library. *Chem. Eur. J.* **2006**, DOI: 10.1002/chem.200600560.
- We use a nomenclature based on the amino acid three letter code to describe 1,3,5-triazepan-2,6-diones. Accordingly, heterocycles prepared from the dipeptide sequence Boc-Xaa-Xbb-OH will be denoted cyclo(Xaa-gXbb-CO). *g* = *gem*, refers to the 2-alkyl *gem*-diamino-derivative of the corresponding amino acid according to the nomenclature proposed by Goodman et al. (*Acc. Chem. Res.* **1993**, *26*, 266–273).
- Rodriguez, M.; Llinares, M.; Doulut, S.; Heitz, A.; Martinez, J. A facile synthesis of chiral N-protected  $\beta$ -amino alcohols. *Tetrahedron Lett.* **1991**, *32*, 923–926.
- Sieber, P. A new acid-labile anchor group for the solid-phase synthesis of C-terminal peptide amides by the Fmoc method. *Tetrahedron Lett.* **1987**, *28*, 2107–2110.
- Pan, Y. H.; Yu, B. Z.; Singer, A. G.; Ghomashchi, F.; Lambeau, G.; Gelb, M. H.; Jain, M. K.; Bahnson, B. J. Crystal structure of human group X secreted phospholipase A2. Electrostatically neutral interfacial surface targets zwitterionic membranes. *J. Biol. Chem.* **2002**, *277*, 29086–29093.
- Jain, M. K.; Yu, B. Z.; Rogers, J.; Ranadive, G. N.; Berg, O. G. Interfacial catalysis by phospholipase A2: dissociation constants for calcium, substrate, products, and competitive inhibitors. *Biochemistry* **1991**, *30*, 7306–7317.
- Volwerk, J. J.; Pieterse, W. A.; de Haas, G. H. Histidine at the active site of phospholipase A2. *Biochemistry* **1974**, *13*, 1446–1454.
- Ancian, P.; Lambeau, G.; Lazdunski, M. Multifunctional activity of the extracellular domain of the M-type (180 kDa) membrane receptor for secretory phospholipases A2. *Biochemistry* **1995**, *34*, 13146–13151.
- Schevitz, R. W.; Bach, N. J.; Carlson, D. G.; Chirgadze, N. Y.; Clawson, D. K.; Dillard, S. E.; Draheim, L. W.; Hartley, N. D.; Jones, E. D.; Mihelich, J. L.; Olkowski, D. W.; Snyder, C.; Sommers, Wery, J.-P. Structure-based design of the first potent and selective inhibitor of human non-pancreatic secretory phospholipase A2. *Nature Struct. Biol.* **1995**, *2*, 458–465.
- Smart, B. P.; Pan, Y. H.; Weeks, A. K.; Bollinger, J. G.; Bahnson, B. J. et al. Inhibition of the complete set of mammalian secreted phospholipases A(2) by indole analogues: a structure-guided study. *Bioorg. Med. Chem.* **2004**, *12*, 1737–1749.
- Dillard, R. D.; Bach, N. J.; Draheim, S. E.; Berry, D. R.; Carlson, D. G.; Chirgadze, N. Y.; Clawson, D. K.; Hartley, L. W.; Johnson, L. M.; Jones, N. D.; McKinney, E. R.; Mihelich, E. D.; Olkowski, J. L.; Schevitz, R. W.; Smith, A. C.; Snyder, D. W.; Sommers, C. D.; Wery, J. P. Indole inhibitors of human nonpancreatic secretory phospholipase A2. 1. Indole-3-acetamides. *J. Med. Chem.* **1996**, *39*, 5119–5136.
- Draheim, S. E.; Bach, N. J.; Dillard, R. D.; Berry, D. R.; Carlson, D. G.; Chirgadze, N. Y.; Clawson, D. K.; Hartley, L. W.; Johnson, L. M.; Jones, N. D.; McKinney, E. R.; Mihelich, E. D.; Olkowski, J. L.; Schevitz, R. W.; Smith, A. C.; Snyder, D. W.; Sommers, C. D.; Wery, J. P. Indole inhibitors of human nonpancreatic secretory phospholipase A2. 3. Indole-3-glyoxamides. *J. Med. Chem.* **1996**, *39*, 5159–5175.
- Dillard, R. D.; Bach, N. J.; Draheim, S. E.; Berry, D. R.; Carlson, D. G.; Chirgadze, N. Y.; Clawson, D. K.; Hartley, L. W.; Johnson, L. M.; Jones, N. D.; McKinney, E. R.; Mihelich, E. D.; Olkowski, J. L.; Schevitz, R. W.; Smith, A. C.; Snyder, D. W.; Sommers, C. D.; Wery, J. P. Indole inhibitors of human nonpancreatic secretory phospholipase A2. 2. Indole-3-acetamides with additional functional-ity. *J. Med. Chem.* **1996**, *39*, 5137–5158.

- (45) Ferrara, P.; Gohlke, H.; Price, D. J.; Klebe, G.; Brooks, C. L., 3rd Assessing scoring functions for protein–ligand interactions. *J. Med. Chem.* **2004**, *47*, 3032–3047.
- (46) Deng, Z.; Chuaqui, C.; Singh, J. Structural interaction fingerprint (SIFt): a novel method for analyzing three-dimensional protein–ligand binding interactions. *J. Med. Chem.* **2004**, *47*, 337–344.
- (47) Hopkins, A. L.; Groom, C. R.; Alex, A. Ligand efficiency: a useful metric for lead selection. *Drug Discovery Today* **2004**, *9*, 430–431.
- (48) Pieper, U.; Eswar, N.; Davis, F. P.; Braberg, H.; Madhusudhan, M. S.; Rossi, A.; Marti-Renom, M.; Karchin, R.; Webb, B. M.; Eramian, D.; Shen, M. Y.; Kelly, L.; Melo, F.; Sali, A. MODBASE: a database of annotated comparative protein structure models and associated resources. *Nucleic Acids Res.* **2006**, *34*, D291–295.
- (49) Scott, K. F.; Graham, G. G.; Bryant, K. J. Secreted phospholipase A2 enzymes as therapeutic targets. *Expert Opin. Ther. Targets* **2003**, *7*, 427–440.
- (50) Laye, J. P.; Gill, J. H. Phospholipase A2 expression in tumours: a target for therapeutic intervention? *Drug Discovery Today* **2003**, *8*, 710–716.
- (51) Reid, R. C. Inhibitors of secretory phospholipase A2 group IIA. *Curr. Med. Chem.* **2005**, *12*, 3011–3026.
- (52) Webb, N. R. Secretory phospholipase A2 enzymes in atherogenesis. *Curr. Opin. Lipidol.* **2005**, *16*, 341–344.
- (53) Triggiani, M.; Granata, F.; Giannattasio, G.; Marone, G. Secretory phospholipases A2 in inflammatory and allergic diseases: not just enzymes. *J. Allergy Clin. Immunol.* **2005**, *116*, 1000–1006.
- (54) Meyer, M. C.; Rastogi, P.; Beckett, C. S.; McHowat, J. Phospholipase A2 inhibitors as potential anti-inflammatory agents. *Curr. Pharm. Des.* **2005**, *11*, 1301–1312.
- (55) Singer, A. G.; Ghomashchi, F.; Le Calvez, C.; Bollinger, J.; Bezzine, S.; Rouault, M.; Sadilek, M.; Nguyen, E.; Lazdunski, M.; Lambeau, G.; Gelb, M. H. Interfacial kinetic and binding properties of the complete set of human and mouse groups I, II, V, X, and XII secreted phospholipases A2. *J. Biol. Chem.* **2002**, *277*, 48535–48549.
- (56) Smart, B. P.; Oslund, R. C.; Walsh, L. A.; Gelb, M. H. The first potent inhibitor of Mammalian group X secreted phospholipase A2: elucidation of sites for enhanced binding. *J. Med. Chem.* **2006**, *49*, 2858–2860.
- (57) Murakami, M. Hot topics in phospholipase A2 field. *Biol. Pharm. Bull.* **2004**, *27*, 1179–1182.
- (58) Murakami, M.; Kudo, I. Secretory phospholipase A2. *Biol. Pharm. Bull.* **2004**, *27*, 1158–1164.
- (59) Jones, G.; Wilett, P.; Glen, R. C.; Leach, A. R.; Taylor, R. Development and validation of a genetic algorithm for flexible docking. *J. Mol. Biol.* **1997**, *267*, 727–748.
- (60) SYBYL 6.91, Tripos Assoc., Inc.: St. Louis, MO.
- (61) Bairoch, A. The ENZYME database in 2000. *Nucleic Acids Res* **2000**, *28*, 304–305.

JM0606589